Executive Summary

Integration of the ESP instrument into the existing Del Mar chain-catenary mooring system by including a stretch-hose between the buoy and the ESP presents some challenges. The resulting depth of the instrument depends strongly on the tension-strain characteristics of the hose which are difficult to predict accurately. Thus, this application of the stretch-hose is novel; typically these components are used in systems that employ a sub-surface float that pulls up on the anchor, meaning that the exact behavior of the stretch-hose is less significant in the mooring behavior.

This report collates all of the available tension-strain behavior for this type of hose. From this data a best estimate envelope of tension-strain behavior for hoses of various lengths has been created. These estimates are then used to set the manufactured length of the stretch-hose that will result in the ESP instrument being as close to 15m depth as possible across the range of expected current and wind loading. The results indicate that once installed, the depth variability with current loading will be relatively small (< 1m). However the accuracy to which the instrument can be placed at 15m is limited to about 3m.

The target depth of 15m for the ESP instrument is approaching the absolute minimum of what is possible with this design. The un-stretched hose length in this case is 7m. Shorter hoses begin to quickly lose their elastic effects as the termination effects begin to dominate.

In this design the static downward loading on the lower end of the hose is set to be about 550lbs. This loading is the sum of the in-water weight of the ESP assembly, the wire-rope and instrumentation, the depressor “pig” weight, and the chain not supported by the seafloor. The weight distribution between the pig weight and the ESP assembly is a variable in the design. Advantages of making the ESP assembly buoyant and concentrating all the required weight in the pig weight is that the wire-rope is biased to a higher tension which reduces the likelihood of zero-tension events in large waves, and the possibility that the ESP instrument will not sink in the event of a catastrophic stretch-hose failure. Unfortunately, a buoyant ESP assembly will be challenging to deploy in an anchor-last procedure without having the ESP lie on its side at some point. For this reason, the design currently splits the wet-weight between the ESP assembly and the pig weight. Designing the ESP assembly to be heavier than water and with sufficient righting moment will make it possible for it to hang below the buoy as the remainder of the mooring is deployed.

Decisions to be made at this point are if the expected depth variability is acceptable and if it’s acceptable to ballast the ESP assembly heavy and risk loss in the case of a stretch-hose failure. If this isn’t acceptable, an anchor first deployment will need to be considered such that the mooring string downward force orients the ESP after it’s in the water. More creative solutions may also be possible, but could complicate the deployment by requiring divers as is the case with current ESP deployments.

ESP Integration into Del Mar Moorings

June 5, 2015

A previous report analyzed a variety of approaches for integrating an ESP into existing moorings at the Del Mar and CCE2 site (*ESP Integration into Existing Del Mar and CCE2 Moorings*). This report provides detailed analysis specific to the chain-catenary design at the Del Mar site. In particular the impact of the stretch hose characteristics and the cage design are examined along with the effects of various current profiles upon the ESP depth.

As previously described, the ESP in its shallow water housing is very massive compared to traditional oceanographic instrumentation. To reduce the dynamic loading this introduces into the chain-catenary mooring design, a compliant element between the ESP and the surface buoy is required. For this application the stretch hoses produced by EOM Offshore are appropriate since they provide an electrical pathway for communications in a component that stretches.

A significant challenge is the variability in the stress-strain behavior of the stretch-hose element. There are three contributions to this variability; manufacturing tolerances, the effects of the terminations upon the assembly, and changes that occur in use. Efforts to characterize this behavior over the years have been limited due to the cost of testing and because the mooring designs these hoses are used in don't have a large sensitivity to the stretch characteristics of the hose (subsurface float designs). For the proposed Del Mar mooring however, the stress-strain behavior of the hose will have a strong influence on the resulting instrument depth and it is therefore important to characterize carefully. For this reason, an analysis of all known existing stress-strain behavior for these components has been performed. This analysis indicates that there is a significant uncertainty in the stress-strain behavior of the hoses and this uncertainty needs to be accommodated in the mooring design as much as possible.

Based on the expected stress-strain behavior of the hose, models of the proposed Del Mar mooring in the expected environmental conditions have been computed. Models of the static mooring position in various current and wind conditions establish an envelope of expected instrument depth for the range of stretch hose behaviors. Time-dependent models have also been run that include the dynamic effects of wave-forcing to predict the minimum and maximum tensions expected in the system.

The primary results of this report are:

- Suggested manufactured length of stretch hose to purchase (7m)
- Requirements on instrument package in-water weight and pig weight to achieve desired instrument depth and dynamic performance. (ESP assembly wet weight = 170lbs, pig weight wet weight = 220lbs)

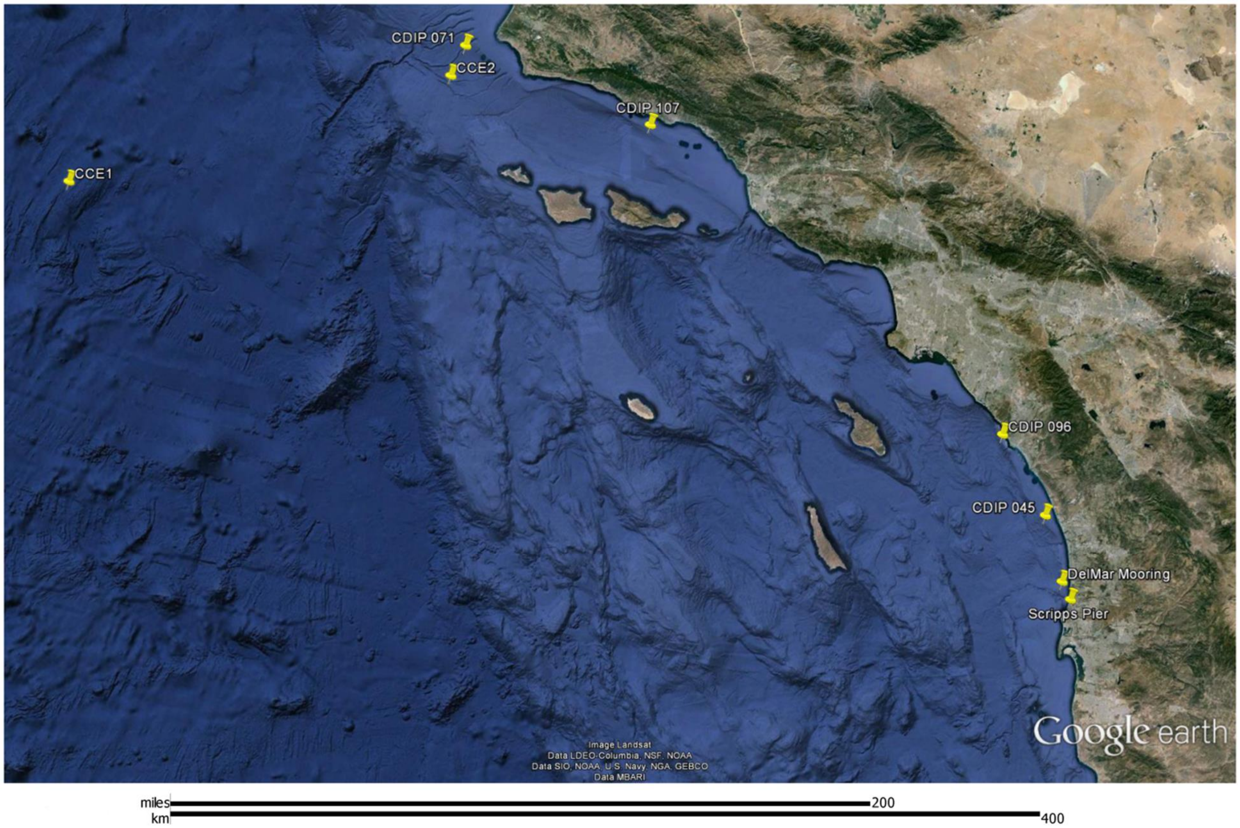

Figure 1: Location in Southern California of Del Mar buoy, CCE2 buoy, and relevant wave measurement sites.

Environment

Figure 1 illustrates the locations of the Del Mar site relative to the location of wave-measurement instrumentation that has been in place long enough to provide some statistics (although none of these have been in place to reliably predict traditional measures such as the sea state present in a storm with an extended return period, i.e. 100 years). CDIP site 045 is likely to provide a reasonable representation of the Del Mar site. Figures in Appendix A illustrate the observed sea state at CDIP 045 over the past 18 years. It is clear that this is an extremely mild location as ocean sites go, in this time the largest observed significant wave height over a 30 minute period was 4.8m with a peak period of 9s. The most common sea state observed is characterized by a significant wave height of 1m with a peak period of 16 seconds. For the dynamic analysis, a 2m significant wave height at 14 seconds is used to represent a nominal condition since the most common condition is so benign.

Wind data has not been collected at these sites. For wind in the subsequent analysis the wind required to create the fully developed significant wave height under consideration will be used (i.e. as per Pierson-Moskowitz). This corresponds to 27kts for the largest observed sea state and 13kts for the most commonly observed sea state.

Measurements of current at the deployment site are illustrated in Figure 2. Shown are the magnitude of the current vectors (direction information is discarded). For the purposes of mooring analysis this is the most convenient since we are interested in estimates of the peak and mean currents. The apparent large currents near the bottom are most likely measurement noise. For the mooring analysis, an approximation of the mean current profile shown here is used, with a multiplicative scaling factor applied to examine the effects of current on the mooring behavior. A scaling factor of about 4 corresponds to the most energetic current profiles seen during the observation period of Nov 2009 to May 2011. In fact, convergence of the numerical models is challenging (i.e. at zero current and wind, there is no unique mooring position that satisfies the balance of force equations that form the basis of the analysis). Therefore, mooring behaviors are only examined down to a current scale factor of 1.4.

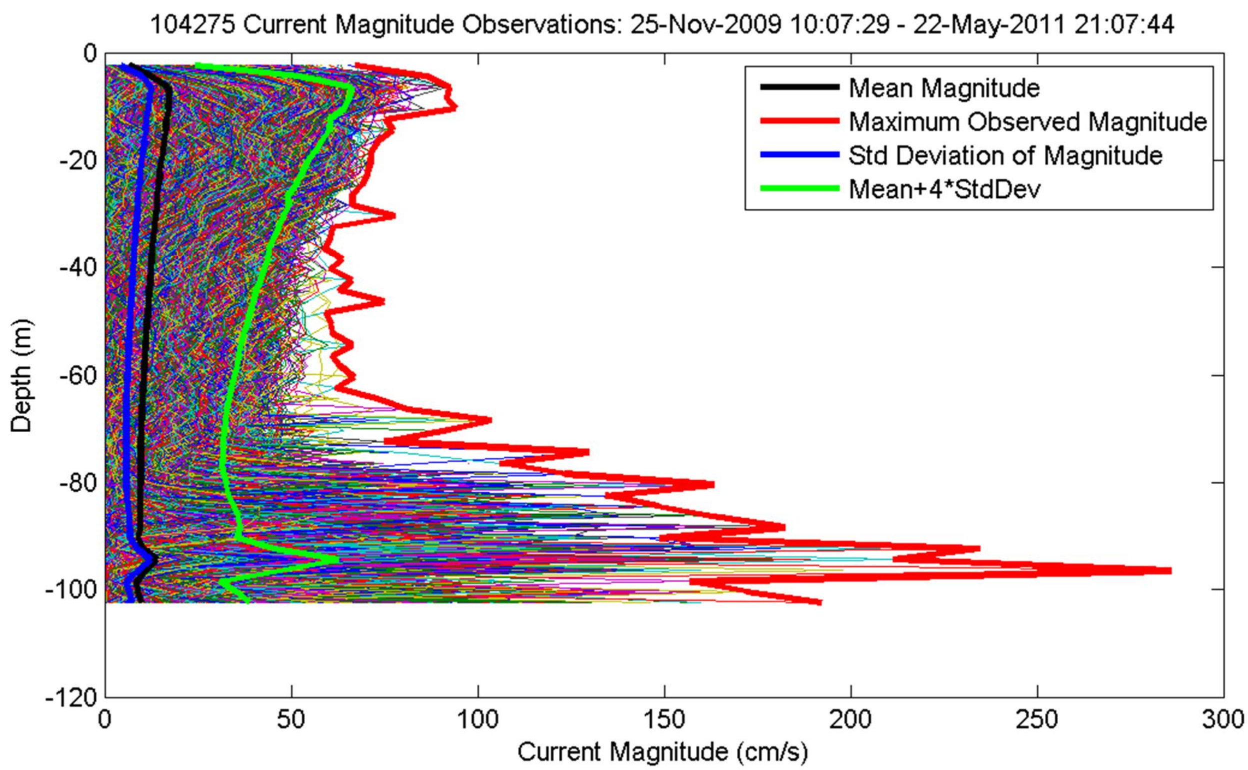

Figure 2 Current profiles measured at Del Mar site.

Stretch Hose Behavior

The tension versus strain behavior of these stretch hoses is difficult to know due to the significant dependence on temperature, cycle rate, time in service, recent tension history and termination effects. Systematic testing to characterize all these effects may be possible, but is almost certainly cost prohibitive. Instead we are left with scattered test data and the need to make some inference about what behaviors to expect for this design.

Most testing and estimates have been made for specific length hoses. Test results are rarely for the same hose length, which makes the results hard to compare due to the effects of the terminations at each end. At the terminations, the hose transitions from its fully compliant behavior to a rigid flange termination over a distance of about 1.9m. Even for the longest hoses made (30m), the termination region is a significant portion of the overall length, and for short test lengths, the terminations dominate the behavior. In 2011, cycle testing was performed on a 4.5m test piece of hose of a design similar to what EOM Offshore is now producing. As part of that testing the hose strain along the test piece was measured at various loadings, allowing the effects of the termination to be characterized. These tests indicate that the strain in the hose varies in a quadratic manner from zero at the ends to that of the fully compliant section at the end of the 1.9m termination section. From this result a relation between the strain of a finite length hose to the strain of the compliant sections alone can be determined. Appendix B shows this analysis and produces the simple relation between the strain of a manufactured length of hose and the compliant section as

$$e_m = (1\text{-}4a/3L_0)\ e_c \tag{1}$$

where e_c is the strain in the compliant section of the hose, e_m is the strain of the entire piece including the terminations, L_0 is the manufactured length, a = 1.9m.

Using this relation, the estimated compliant tension-strain behavior from all known tests and estimates has been plotted in Figure 3. The heavy green, black, and red lines are best estimates of the envelope of tension-strain behavior to be expected and are intended to be used as guidance for new designs. These estimates have been made somewhat subjectively and the envelope doesn’t include the results from all tests. In particular, the very stiff estimates made by Grosenbaugh for the AST hoses were not actual tests, but instead where made by looking at the buoy position versus measured tension data for a test deployment. Subsequent modelling of the mooring to determine what hose stiffness would have been required to create those buoy positions are the origin of the tension-strain curves here. Unfortunately, that report is not clear if the overall hose stretch is reported, or that of the compliant section only. Additionally, there are a lot of other systematic biases that could have made the hoses appear stiffer than they are so this data has been treated as an outlier. At the other extreme, the 2011 tests indicate that the hoses are quite a bit softer. The best estimate envelope excludes these data for a number of reasons. In particular, those tests were run inside at relatively elevated temperature compared to at-sea conditions, there was little cooling of the hose during the cycling compared to an at-sea situation, some delamination of the test piece terminations was observed during the tests which allowed one part of the hose to stretch further than normal, and the test piece was subjected to large constant tensions periodically throughout the cycling to measure the strain distribution along the hose as previously described.

The figure legend includes a polynomial estimate of tension-strain behavior for the minimum, nominal, and maximum envelop. To use these curves as estimates for a finite length hose, equation (1) needs to be solved for e_c and the result inserted into the polynomial to provide a relation between overall strain and tension.

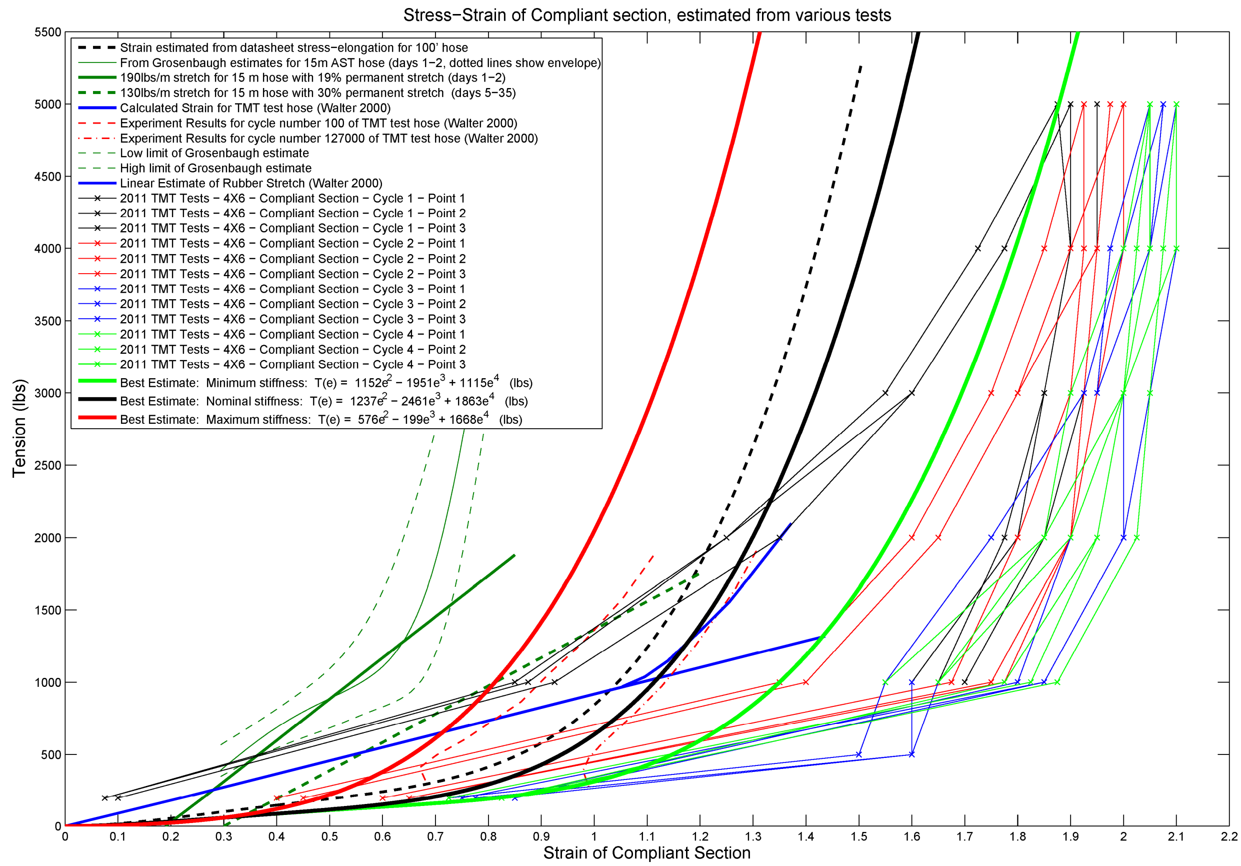

Figure 3 Compilation of all available tension-strain estimates of the stretch hose design to be used in the Del Mar mooring. To provide a consistent basis for test items of different lengths, the results are plotted against the strain of only the compliant section of the hose. e.g. the end effects of the terminations have been removed.

Mooring Design and Static Analysis

Figure 4 illustrates the existing mooring deployed regularly at the Del Mar site. The approach for this deployment is to retain the chain-catenary mooring design and to insert the ESP instrument into this existing mooring and to add a stretch-hose between the ESP instrument frame and the surface buoy.

Figure 5 illustrates the proposed mooring design. This arrangement creates a strong correlation between the tension-strain behavior of the stretch hose and the resulting instrument depth. In order to characterize what to expect, static modeling runs have been performed that compute the instrument depth that results from varying current and wind forcing for the three stretch-hose behavior estimates (soft, nominal, and stiff). Figure 6 shows these results for the case where the ESP and frame is ballasted to be 170lbs heavy in water, and a 220 lb depressor weight is included. As can be seen, the ESP instrument mean depth will vary relatively little (<1m) through the expected current range, and the uncertainty in the stretch-hose stiffness will limit the accuracy at which the instrument can be placed to +/- 1.5m.

These results are for a case in which no adjustments of the ESP or depressor weight is made to account for the actual measured tension-strain behavior of the hose after it is manufactured. In principle it will be possible to measure the tension-strain behavior and adjust the weights some to refine the instrument depth. In practice this could be challenging due to the above mentioned challenges in measuring the tension-strain behaviors (temperature dependence, load-history dependence).

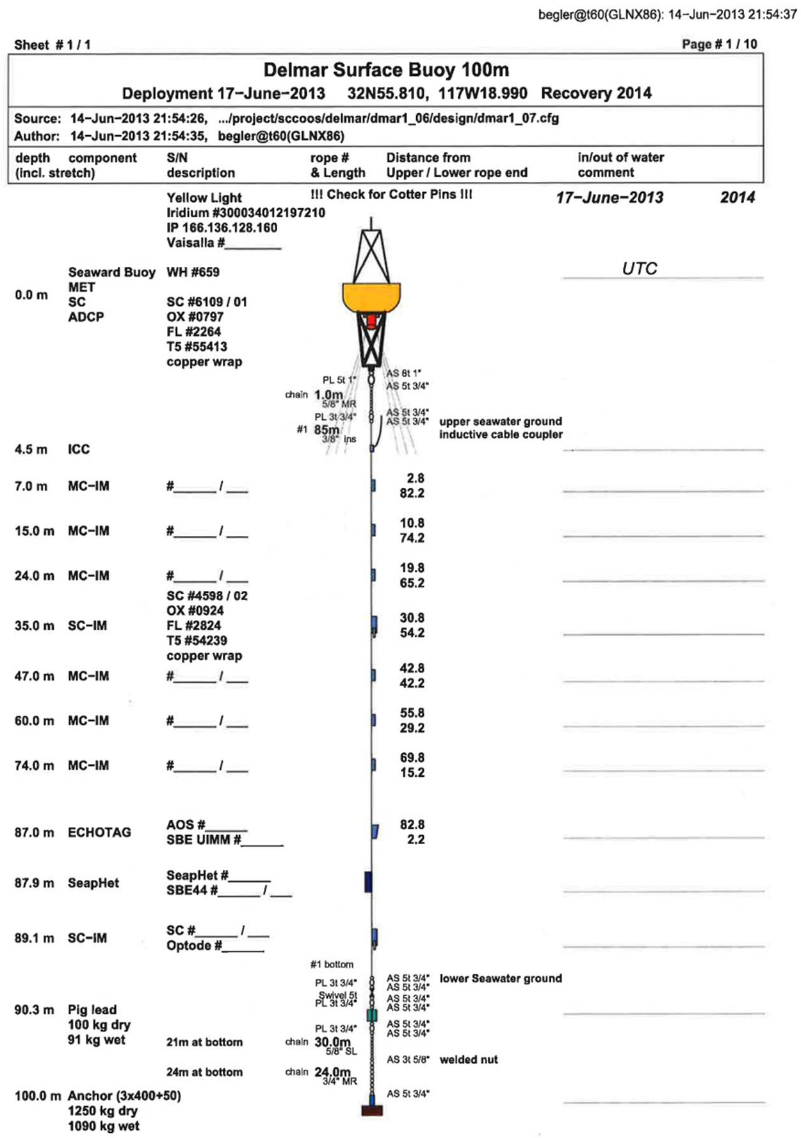

Figure 4: Layout of existing Del Mar mooring in 100m of water.

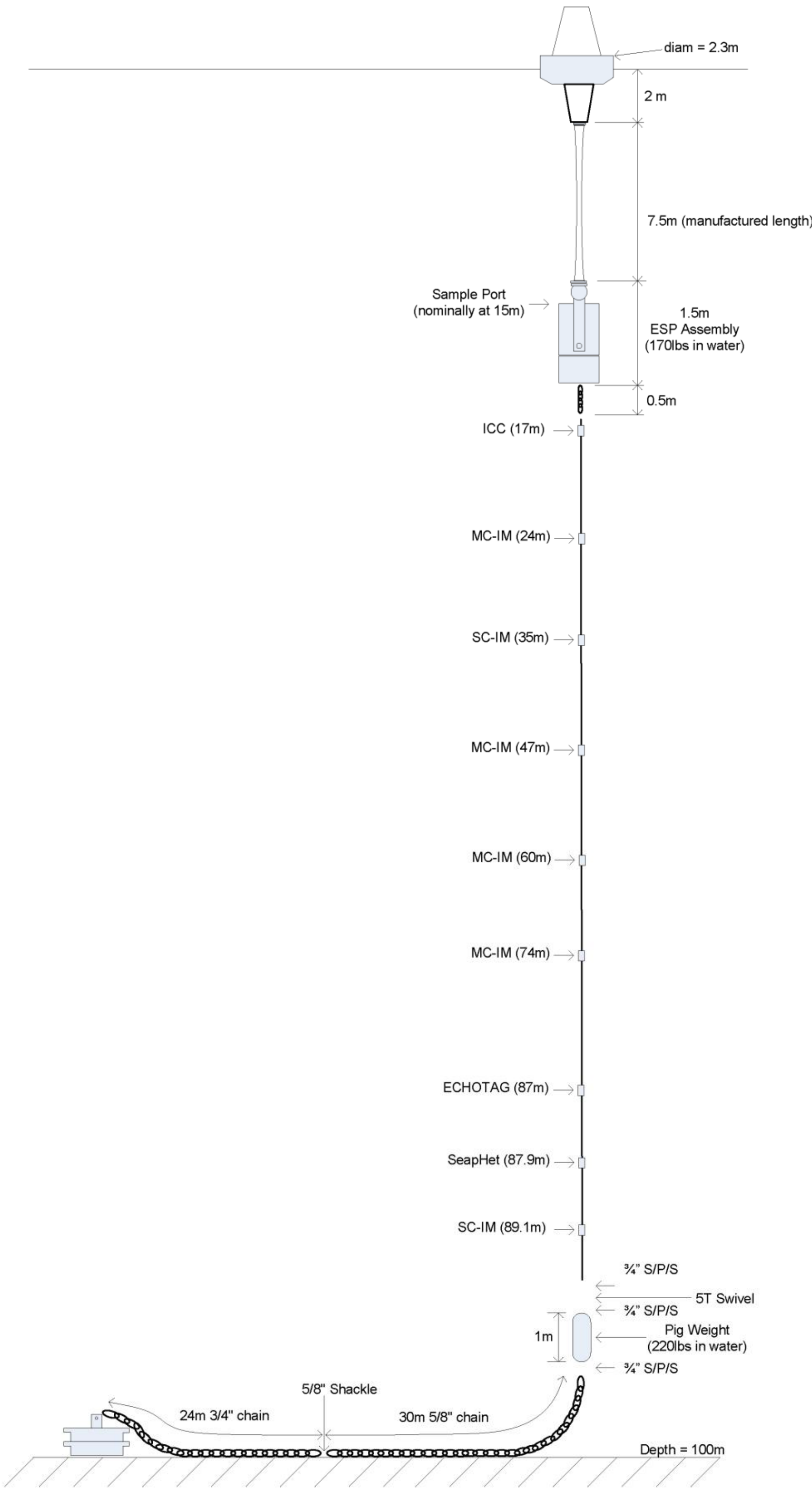

Figure 5 Layout of proposed mooring that includes the ESP assembly at the Del Mar site.

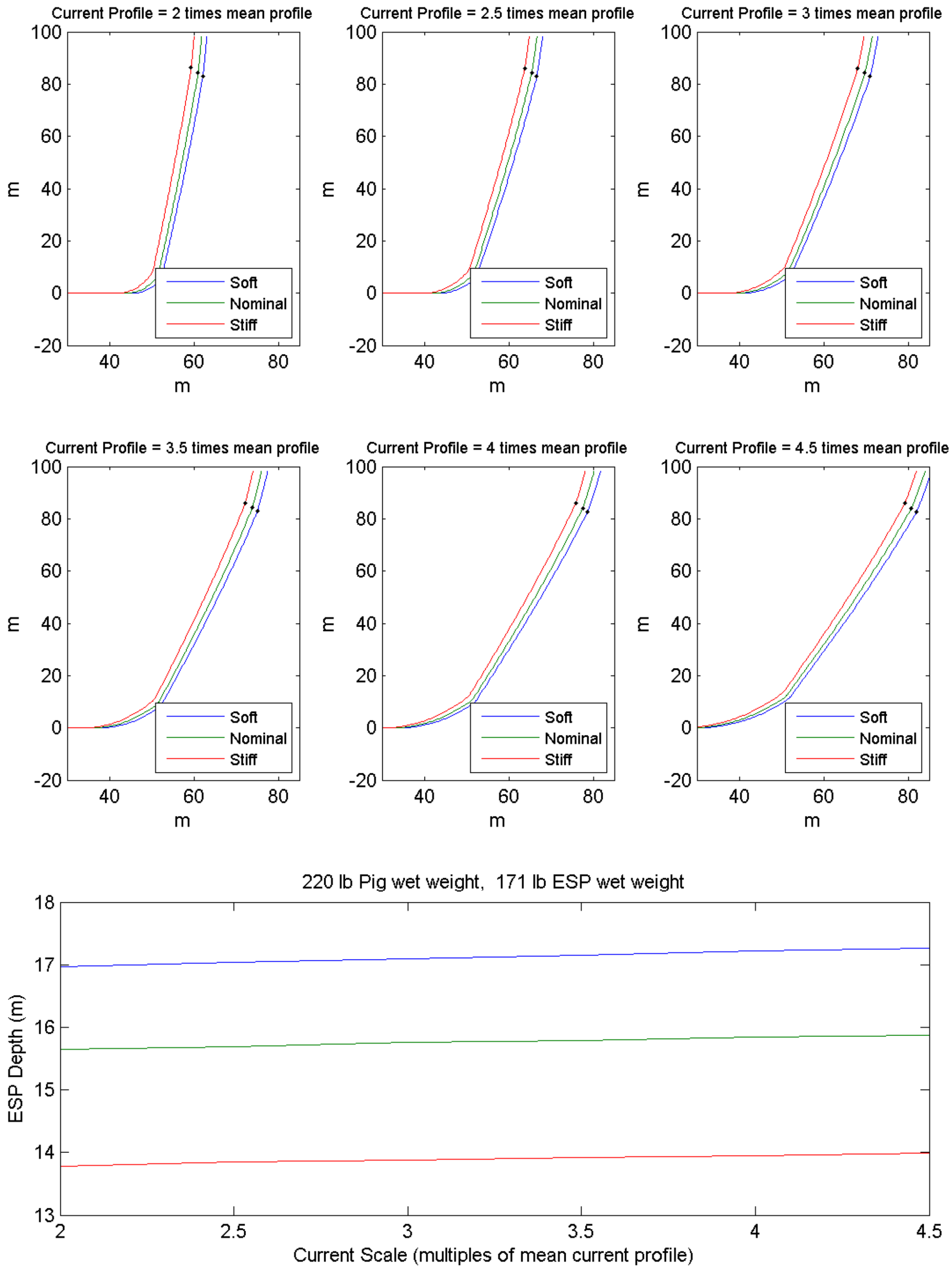

Figure 6 Instrument depth variability due to currents and stretch-hose tension-strain relationship.

Dynamic Analysis

The results in the previous section are driven only by constant current and wind forcing. The dynamic response of the system to wave-forcing is also important and the numerical modeling performed includes wave forcing for two sea states, moderate and extreme as described above.

Figure 7 and Figure 8 show the expected tensions in various parts of the mooring for the extreme and moderate sea state. Each figure shows the effects of distributing the wet-weight differently between the ESP assembly and the pig weight. The top pane in each figure shows the results for a slightly buoyant ESP, which relies upon the pig-weight entirely to elongate the stretch hose. The middle pane splits the wet-weight and the bottom pane shows the results when the wet weight is concentrated in the ESP assembly.

The advantage of a buoyant ESP is that the mean tensions in the wire below the ESP are higher, reducing the chances for a slack condition. Additionally, if the stretch-hose were to fail, the ESP would remain floating at a depth above its crush depth. The significant disadvantage of this design is that during an anchor-last deployment, it will be difficult to ensure the ESP assembly remains upright before the mooring line tension is in place.

For the proposed design, the wet-weight is split between the ESP and the pig weight in order to address the deployment issue, and maintain some tension in the wire below the ESP. If an anchor-first deployment is possible, this could be revisited.

Figure 9 shows the expected ESP depth in the extreme sea state. This response is not sensitive to the weight distribution of the mooring.

Notable in the dynamic results is a relatively high frequency ringing evident in the segment between the ESP assembly and the pig weight. This feature is due to an excitation of the resonance of the spring-mass system created by the slightly stretchy wire-rope connecting the two masses. This may or may not be present in the physical system, the wire-rope also has some structural damping that will limit this behavior. When such damping is included in the system model, the high frequency signal disappears, but the results shown here do not include this parameter.

Appendix D shows the results for all the various combinations.

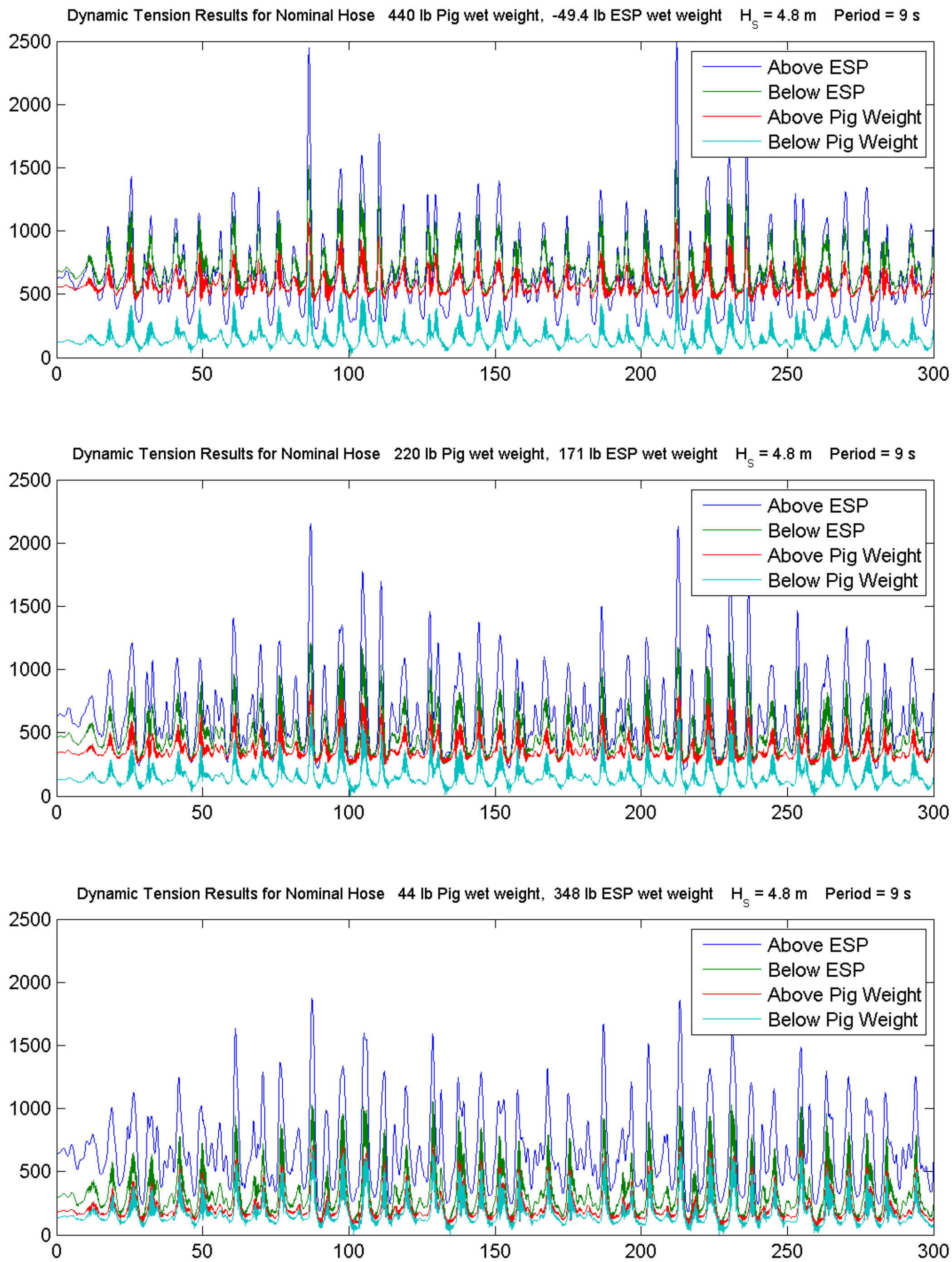

Figure 7 Dynamic tension results for three distributions of wet-weight between the ESP assembly and the pig weight, in the extreme sea state.

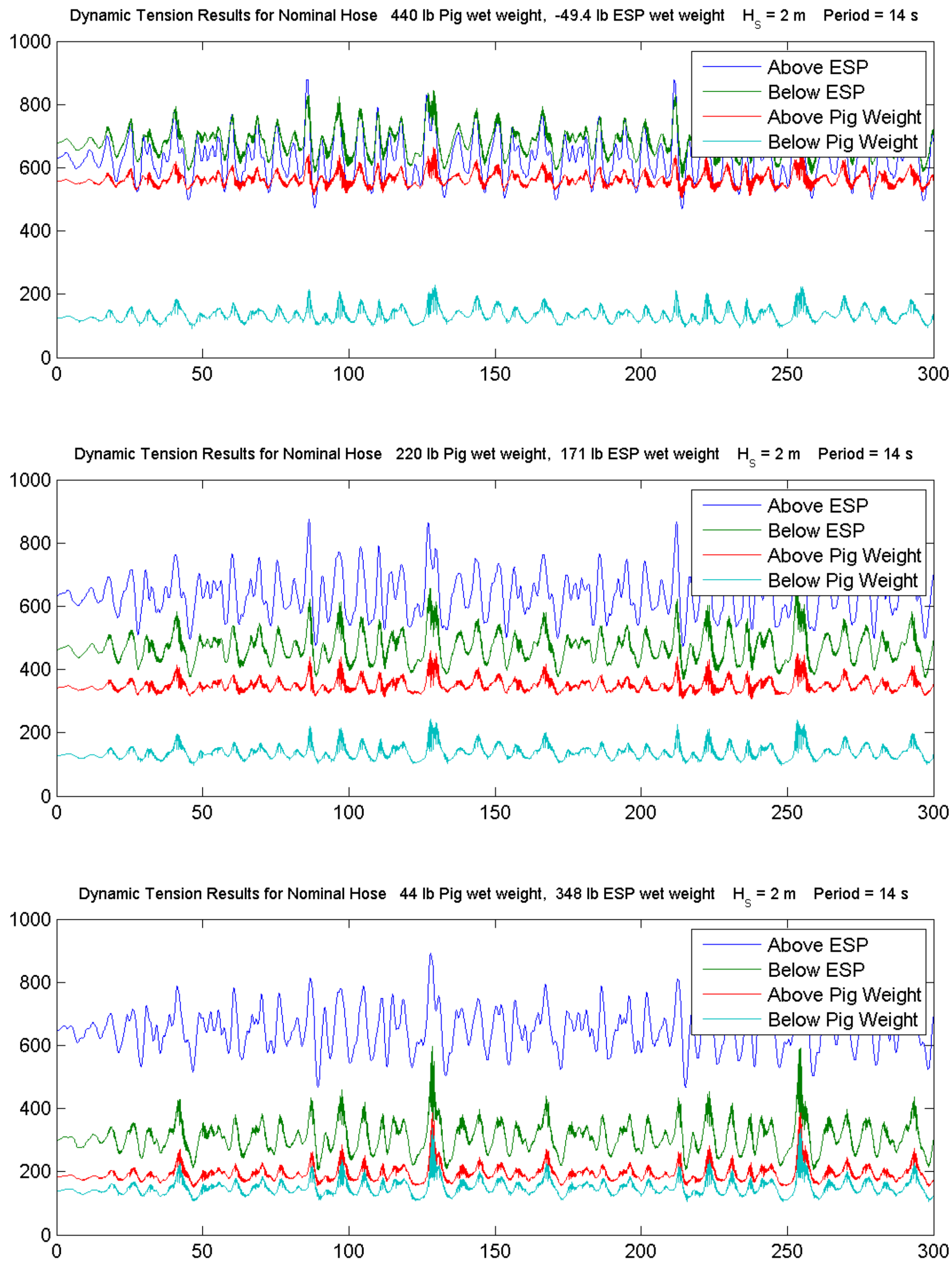

Figure 8 Dynamic tension results for three distributions of wet-weight between the ESP assembly and the pig weight, in the moderate sea state.

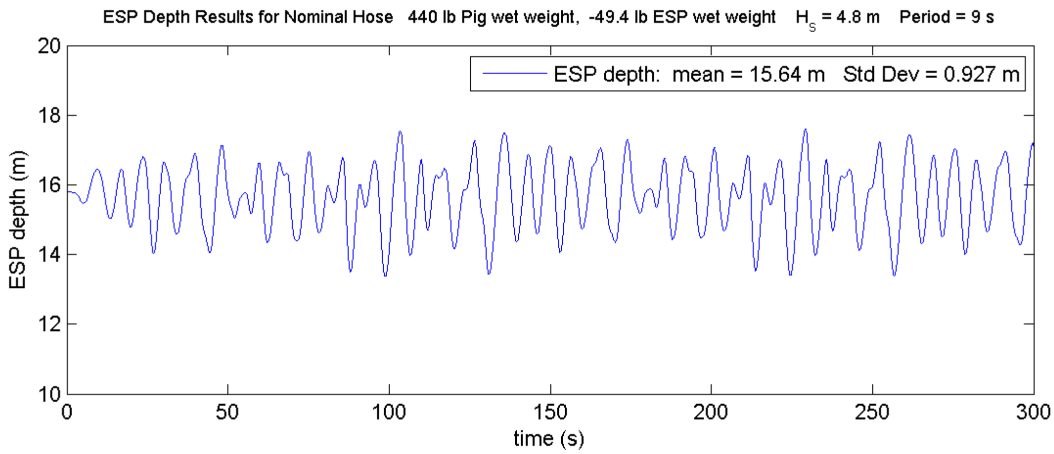

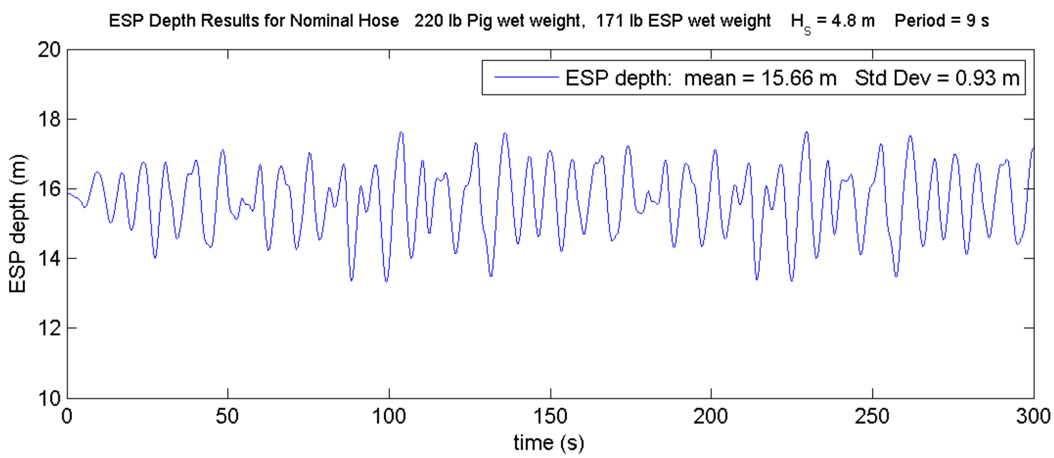

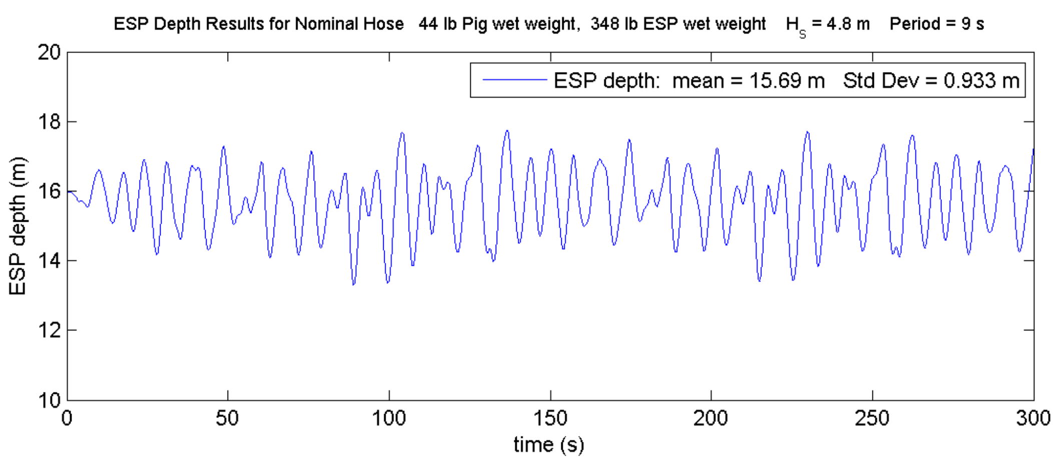

Figure 9 ESP depth response for the extreme sea state.